Journal of Multidisciplinary Engineering Science and Technology (JMEST)
ISSN: 3159-0040
Vol. 2 Issue 3, March - 2015

Characteristics of Focusing Behavior of Virtual Lens with Variable Diameter

Ahmed M. D. E. Hassanein
Systems and Information Department, Engineering Division,
National Research Centre (NRC),
Dokki, Giza, Egypt
Email: ahmed22@aucegypt.edu

***Abstract*—The virtual confocal microscope method is used in microwave imaging to examine the biological tissues. The method depends on focusing the incoming scattered waves from a body to form an image using a virtual lens. A mathematical relationship is found that gives only the possible allowed values for the diameter of the lens for each specific wavelength, minimum required resolution and distance from lens to image. Each of the values of the diameters when used produces images with best quality. Here, we continue on previous work to study the characteristics of the efficiency of the lens in producing images as two parameters are varied. One parameter is the diameter of the virtual lens. Another parameter is the minimum resolution which is required for the calculated images. The efficiency obeys a harmonic behavior as the diameter of the virtual lens changes. Moreover for a constant wavelength, as the minimum required resolution decreases the allowed diameters for the virtual lens to obtain images with good quality become wider.**

Keywords— Harmonic Frequency; Virtual Confocal Microscope; Image Intensity; Resolution; Saturation Curve

I. INTRODUCTION

One of the most successful techniques to detect malign tissues is microwave imaging because it depends on the contrast in dielectric properties between malign and benign tissues [1]. KUBÍNOVÁ et al present in [2] a detailed study and short reviews of confocal imaging and three-dimensional image analysis. Methods for automatic measurement of the characteristics of geometrical microscopic structures, based on 3-D image processing or surface triangulation, are discussed and compared. Three-dimensional reconstruction programs and software implementation of digital methods as well as their practical applications are presented in [2].

Confocal microscopy has emerged to become a useful and efficient tool for imaging human tissue. In [3], a high-performance confocal system that can be easily adapted to an existing light microscope or coupled with an endoscope for remote imaging is designed. The system employs spatially and temporally patterned illumination. In [4], laser scanning confocal microscopy has been proven to become an invaluable tool for a wide range of investigations in the biological and medical sciences for imaging thin optical sections in living and fixed specimens. In [1], the Virtual Confocal Microscope (VCM) method is presented to be used with microwave frequencies to detect cancer. Its success has been proven both theoretically and experimentally in obtaining cross sectional images of different bodies [5].

The performance of the lens which is used in the confocal microscope is of great importance. It defines the ability of the microscope to produce images with high resolution for the object being imaged. In [6], defocusing of a lens has been proven to change the size and intensity distribution of the unit image point. In [7], the performance of a single bi-plano lens that uses low-dispersive radial gradient-index material is evaluated. The dispersion property has been investigated as well. In [8], the beam focusing characteristic of a plasmonic lens (PL) is evaluated. PL is a promising photonic device which makes use of the surface plasmon wave. The surface plasmon wave can be focused using a PL structure for imaging. In [9], quasi-optical imaging systems are shown to require low blurring effect and large depth of focus to obtain an acceptable sharpness of the image. The characteristics of the lens which is used in this type of imaging such as beam spot size and spatial resolution are analyzed both theoretically and experimentally [9].

In [1], the view angle of the virtual lens which is used in the VCM method is modified so as to improve the resolution of the obtained images. A mathematical relationship is found that relates the values of the diameter of the virtual lens to the distance between the lens and the image plane. The possible allowed values for the diameter of the lens are tabulated to image a proposed one dimensional object. The proposed calculated values for the diameter have been proven to improve the quality of the obtained images significantly. The proposed modification has proved to be a success in improving the resolution of the obtained images. Improving the quality of images in examining the human body helps in increasing the probability of detecting illnesses in there early stages and so increasing the chances of curing them.

In this piece of work, we further investigate the nature of the change in the resolution of the virtual confocal microscope as the diameter of the virtual lens is changed. In section two, the mathematical background that is needed for the investigation is

explained. A way to numerically assess how much an image resembles the object being imaged is given. The intensity of an image formed by the virtual confocal microscope method is redefined. An equation for the frequency of the change in intensity is derived. In section three, the efficiency of the method is plotted against changing the diameter of the virtual lens. The effect of changing the minimum required resolution on the efficiency of the method is studied. Finally, a conclusion for all the work done is given. A discussion of the importance of the results and their meaning is shown.

II. MATERIALS AND METHODS

In this section, we study mathematically the characteristics of the VCM method. In one subsection, the theoretical background which is required to clarify the work presented here is shown. In another subsection, the intensity of an image is redefined in simple mathematical terms. Later, an equation to describe how efficiently the method is in producing a replica of an object is given. The equation depends on the difference in intensity between the object used and the images produced.

A. Mathematical Background

The main mathematical equations which describe the virtual confocal microscope method and how changing its diameter can be implemented are shown in [1]. Here, we select the equations which serve our aim in this paper. An image $U_i(u,v=0)$ can be calculated for the object $U_O(\xi,\eta=0)$ using the convolution [10]:

$$U_i(u,v=0)=\int_{-\infty}^{\infty}U_O(\xi,\eta=0)h(u,v=0;\xi,\eta=0)d\eta \quad (1)$$

the function $h(u,v=0;\xi,\eta=0)$ takes the following form [10]:

$$h(u,v=0;\xi,\eta=0)=\frac{1}{\lambda^2 z_1 z_2}\int\exp\left\{\frac{-j2\pi}{\lambda z_2}[(u-M\xi)x]\right\}dx \quad (2)$$

where λ is the wavelength, z_1 is the distance from object to lens, z_2 is the distance from lens to image, ξ is the object axis, u is the image axis, x is the lens axis and M is the magnification of the lens used. In order to obtain a replica of the object, we need to maximize the real part of eq (2). At maximum, the diameter of the virtual lens (x) is [1]:

$$x=\frac{n\lambda z_2}{(u-M\xi)x} \quad (3)$$

where $n=0,1,2,3,4,\ldots\ldots$

From eq (2), the intensity of an image and frequency of the intensity for the VCM method are deduced.

B. Intensity Components

The exponential part in the 1-D solution (eq (2)) can take the form [1]:

$$\exp\left\{\frac{-j2\pi}{\lambda z_2}(u-M\xi)x\right\}=\cos\left[\frac{2\pi}{\lambda z_2}(u-M\xi)x\right]+j\sin\left[\frac{2\pi}{\lambda z_2}(u-M\xi)x\right] \quad (4)$$

Then, the intensity of the exponential part is:

$$I=\left|\exp\left\{\frac{-j2\pi}{\lambda z_2}(u-M\xi)x\right\}\right|^2=\cos^2\left[\frac{2\pi}{\lambda z_2}(u-M\xi)x\right]+\sin^2\left[\frac{2\pi}{\lambda z_2}(u-M\xi)x\right] \quad (5)$$

The intensity I of any calculated image $U_i(u,v=0)$ is equal to the sum of two terms. The square of the cosine term and that of the sine term are added together. Later in our calculations, the object being imaged starts with an amplitude equal one and phase equal zero. Maximizing the cosine term means producing a replica of the object since it represents the real part of the image. To maximize the cosine term which is shown in eq (4), we need to make:

$$\left[\frac{2\pi}{\lambda z_2}(u-M\xi)x\right]=2n\pi \quad (6)$$

However, the value of the intensity for an image is composed of the real and the imaginary parts added together so we need to see how to maximize the imaginary part as well.

To maximize the sine (imaginary) term, we need to make:

$$\left[\frac{2\pi}{\lambda z_2}(u-M\xi)x\right]=\left(\frac{2n+1}{2}\right)\pi \quad (7)$$

C. Evaluation Method

In this subsection, a simple method which can be used to evaluate how good an image resembles the object being imaged is explained. An example is shown in fig 1 to clarify the method. An object which is composed of a line of point sources that have a length of 0.04 m is shown in fig 1a. The Point sources have uniform amplitude equal to one. They are phase locked together and are placed along a line on the ξ axis as shown. This object is used in all the calculations and examples which are shown in this paper. The intensity I which is plotted for the object shown in fig 1a is calculated using:

$$I_O=|U_O(\xi,\eta=0)|^2 \quad (8)$$

An example of a possible image for the object shown in fig 1a is shown in fig 1b. As seen visually, the image is not a good representation of the object being

imaged. The intensity I which is plotted for the image is calculated using:

$$I_i = |U_i(u, v=0)|^2 \quad (9)$$

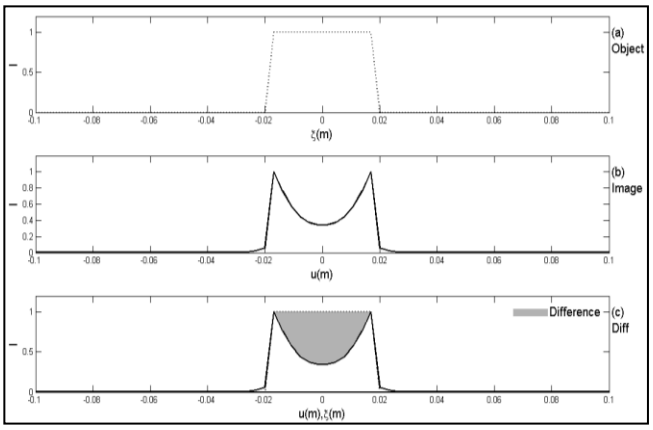

Fig. 1. *: (a) The intensity of an object composed of an array of point sources with an amplitude equal one aligned along the ξ axis. (b) The intensity of a possible image for the object which is shown in fig 1a. (c) The difference in intensity between the object which is shown in fig 1a and its image which is shown in fig 1b is shown in gray color.*

As shown in fig 1c, the difference in area between the intensity of the image and that of the object is taken to be a representation of how good the image resembles the object. As shown, the gray area is equal to the mismatch in imaging the object which is shown in fig 1a. The Efficiency (eff) equation which is used for this cause is:

$$eff = -\sum |I_i - I_O| \quad (10)$$

The result of this equation is either a zero or a negative value. The zero value represents a prefect matching between the image and the object. But, the greater the negativity of the eff, the higher the mismatch between the image and object being imaged is.

III. RESULTS

In this section, Matlab™ is initiated to perform the calculations which are shown here. In the first subsection, the performance of the focusing effect of the virtual lens is evaluated as the diameter is changed. In the second subsection, the characteristics of the efficiency eff of the virtual lens in forming images as the diameter is changed is studied at three different values for the term $(u-\xi)_{\min}$. The calculated results are plotted and explained.

A. Characteristics for a Range of Diameters

For the value $(u-\xi)_{\min} = 0.0031$ m, eq (10) is used to plot the graph in fig 2a. The wavelength which is used in our calculations is $\lambda = 0.006$ m. The distance between the lens and corresponding image is $z_2 = 0.2$ m. The amplification ratio for the lens is $M = 1$.

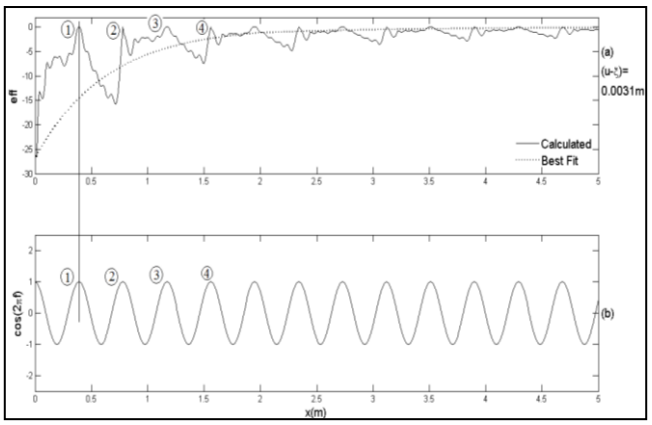

Fig. 2.*: (a) The efficiency of the virtual confocal microscope (eff) is plotted against a change in the diameter of the virtual lens (x). (b) The magnitude of the $\cos(2\pi f)$ is plotted against a change in the diameter of the lens (x).*

TABLE I. : RESULTS WHICH ARE SHOWN IN FIG 2A ARE TABULATED.

peak #	spike/curve	n value	n	x(m)
1	Curve	1	Odd	0.39
2	Spike	2	Even	0.78
3	Curve	3	Odd	1.17
4	Spike	4	Even	1.56

The real term in eq (2) defines the diameter x to be used to obtain the images with the best resolution as is shown in eq (3). The results which are shown in fig. 2a are tabulated in table I. In fig 2a, the first four peaks with the highest eff are numbered consecutively. We can find that the first and third peaks are calculated using odd values of n. The shape of the peaks is smooth and rounded at the top. But, the second and fourth peaks are calculated using even values of n. The shape of the peaks is steep and pointed in the form of a spike at the top.

The reason can be seen when eq (6) and eq (7) are inspected. The n term in the numerator of eq (6) forms odd and even multiples of 2π, but the $2n+1$ term in the numerator of eq (7) forms only odd multiples of $\frac{\pi}{2}$. The odd values satisfy both equations so that the cosine as well as the sine terms interplay a role in maximizing the eff. The shape of the curve around the odd values of n is smooth with no spikes. But for even values, the cosine term only is satisfied and so it plays alone the role of maximizing the eff. That is why, the curve forms a spike at the n point which satisfies the cosine term only. In other words, the lack of satisfying the sine term is the reason for the appearance of these spikes.

As shown in fig 1a, the efficiency eff curve oscillates between maximum and minimum values. The magnitude of the oscillations fades out as the diameter of the virtual lens x increases. The curve saturates to maximum eff as the value of x increases. Next, Matlab™ is used to get the best fit of the curve. The curve fits best an exponential function as shown in fig 2a (dotted line). So, we assume the function to take the form:

$$J(K) = Ae^{(-BK)} \tag{11}$$

where J is the dependent variable, K is the independent variable, A is a starting constant and B is rate of saturation constant.

The best fit in fig 2a (dotted line) has the following function:

$$eff = -25.5882e^{(0.7813x)}$$

The function increases in value until it saturates at $eff = 0$. The rate by which the curve saturates to maximum efficiency is $0.7813\,\mathrm{m}^{-1}$.

The oscillations of the efficiency eff curve are seen to repeat. Next, the harmonic frequency by which the results of the efficiency curve behaves is deduced. The real part of eq (4) is:

$$\cos\left[\frac{2\pi}{\lambda z_2}(u - M\xi)x\right] \tag{12-a}$$

The harmonic oscillations can be represented by another cosine function which can be defined in terms of frequency f such as:

$$\cos(2\pi f) \tag{12-b}$$

where f is the frequency of the cosine wave. By comparing eq (12-a) and (12-b), we can find an equation for f as follows:

$$f = \frac{(u - M\xi)x}{\lambda z_2} \tag{12-c}$$

where f stands for the frequency at which the focusing effect of the virtual lens happens. Eq (12-b) is used to plot the graph in fig 2b. The first four crests are numbered consecutively. A vertical line is drawn at the peak of crest one in fig 2b. The line is seen to pass through the first peak of the eff curve in fig 2a. The four peaks in fig 2a and the four crests in fig 2b stands at the exact values of the diameter x. The cosine function in eq (4) dictates the main focusing behavior of the virtual lens in spite of the fact that the intensity of an image depends on both cosine and sine terms.

B. Characteristics when Changing Resolution

In this subsection, the same values which are mentioned at the start of the previous subsection are used in calculating eq (10) to plot the graphs in fig 3. But here, the values $(u-\xi)_{\min} = 0.0041\,\mathrm{m},\ 0.002\,\mathrm{m}$ and $0.001\,\mathrm{m}$ are used in figs 3a, 3b and 3c consecutively. The first four peaks of eff are numbered in each of the three subfigures.

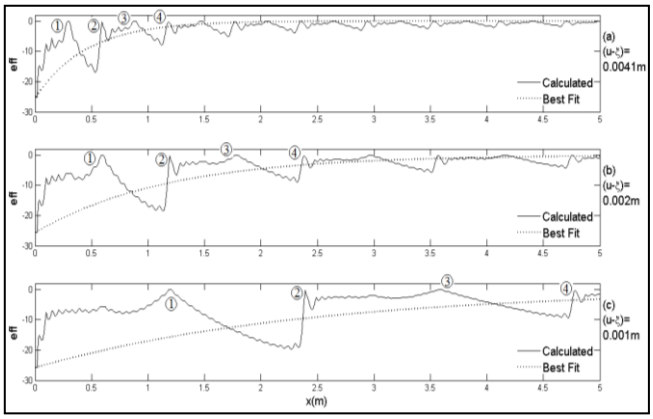

Fig. 3.: *(a) The efficiency (eff) is plotted against changing the diameter of the virtual lens (x) for different values for the parameter $(u-\xi)$. (a) $(u-\xi)_{\min} = 0.0041$ m. (b) $(u-\xi)_{\min} = 0.002$ m. (c) $(u-\xi)_{\min} = 0.001$ m.*

The x values of the diameter of the virtual lens for each of the four peaks in the three subfigures are tabulated in table II.

TABLE II. : RESULTS WHICH ARE SHOWN IN FIG 3 ARE TABULATED.

peak #\ $(u-\xi)_{\min}$	0.0041	0.002	0.001
1	0.29	0.59	1.19
2	0.59	1.19	2.39
3	0.88	1.78	3.58
4	1.18	2.38	4.78

For $(u-\xi)_{\min} = 0.0041\,\mathrm{m}$, the first four peaks stands at $x = 0.29\,\mathrm{m},\ 0.59\,\mathrm{m},\ 0.88\,\mathrm{m}$ and $1.18\,\mathrm{m}$ respectively. For $(u-\xi)_{\min} = 0.002$ m, the first four peaks correspond to lens diameters $x = 0.59\,\mathrm{m},\ 1.19\,\mathrm{m},\ 1.78$ m and 2.38 m respectively. For $(u-\xi)_{\min} = 0.001$ m, the first four peaks stands at $x = 1.19\,\mathrm{m},\ 2.39\,\mathrm{m},\ 3.58\,\mathrm{m}$ and $4.78\,\mathrm{m}$ respectively.

As higher resolution is required, the interspacing between the calculated values for the diameters of the virtual lens increases. In order to produce images with minor details, more scattered waves are needed to form the image and so wider diameters for the virtual lens are required.

Matlab™ is used to obtain the best fit for each of the curves which is shown in fig 3. Each of the curves fits best with an exponential function as shown in fig 3 (dotted lines). Each curve fits a function which has the same form as that stated in eq (11).

First, the best fit in fig 3a (dotted line) matches with a function which has the following form:

$$eff = -25.1790e^{(1.1016x)} \quad (13)$$

Second, the best fit in fig 3b (dotted line) matches with a function which has the following form:

$$eff = -25.6323e^{(0.4307x)} \quad (14)$$

Third, the best fit in fig 3c (dotted line) matches with a function which has the following form:

$$eff = -25.8345e^{(0.2087x)} \quad (15)$$

When examining the values of B in the three functions, we find that the highest rate by which a curve saturates to maximum efficiency is seen in eq (13) followed by eq (14) followed by eq (15). The values of the minimum required resolution $(u-\xi)_{\min}$ are the reason for this decreasing order in the values of B. The higher the resolution that is required, the wider the diameter of the lens that is needed to obtain images with good quality. The wider the diameter of the lens, the more scattered waves which are collected from the object and so the more information that is collected about the object being imaged.

C. *Two Worst Cases for Resolution*

In this subsection, the minimum efficiency eff is examined to see how badly the resolution can be. We discuss the two cases which are plotted in fig 3a and 3c. The first is where the minimum resolution required $(u-\xi)_{\min} = 0.0041$ m is larger than half the wavelength used $\lambda = 0.006$ m. The worst scenario for this case can be found by locating the minimum eff for the curve plotted in fig 3a. At $x = 0.53$ m, the minimum eff is found between the first and second peaks. The minimum eff which is formed at $x = 0$ is disregarded because it is an impractical value for the diameter. The object being imaged and its image which is calculated using the diameter $x = 0.53$ m are plotted in fig 4. The difference between the intensities of the object and its image is shown in gray color.

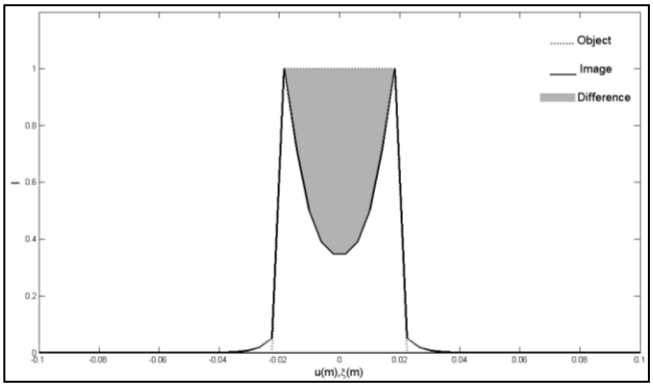

Fig. 4.*: The object (dotted line), its image (solid line) and the difference between the intensities of both of them (gray area) are shown.* $(u-\xi)_{\min} = 0.0041$ *m,* $x = 0.53$ *m.*

The second is where the minimum resolution required $(u-\xi)_{\min} = 0.001$ m is smaller than half the wavelength used $\lambda = 0.006$ m.

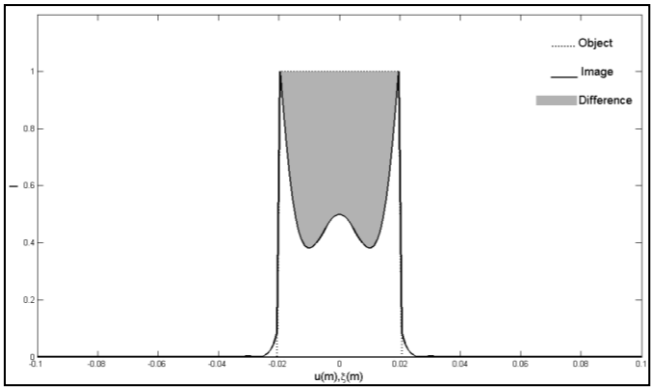

Fig. 5.*: Same as fig 4.* $(u-\xi)_{\min} = 0.001$ *m,* $x = 2.27$ *m.*

At $x = 2.27$ m, the minimum eff is found between the first and second peaks as well. The object being imaged and its image which is calculated using the diameter $x = 2.27$ m are plotted in fig 5. The difference between the intensities of the object and its image is shown in gray color as well. By comparing fig 4 and fig 5, we can see that the gray area in fig 5 is larger than that in fig 4. This fact can be foreseen by examining eq (13) and eq (15). The values of A in both equations represent the starting minimum value at $x = 0$ for the best fit. The value of A for the curve in fig 3c is smaller than that in fig 3a. This indicates that the minimum values which are seen in fig 3c is smaller than the corresponding ones found in fig 3a. Also, the higher minimum resolution required in fig 3c than that in fig 3a dictates less minimum efficiency except at very wide diameters.

IV. Discussion and Conclusion

The virtual confocal microscope method uses microwave frequencies to detect cancer. In previous studies [1], the view angle of the virtual lens which is used in the method is modified so as to improve the resolution of the obtained images. A mathematical relationship is found that relates the values of the diameter of the virtual lens to the distance between the lens and the image plane. The proposed calculated values for the diameter improve the quality of the obtained images significantly. Furthermore in this paper, the new modification is scrutinized to know the advantages of using it. Two parameters are varied to see their effect on the resolution of the obtained images. A tool is introduced to evaluate how much an image resembles the object being imaged. The tool which is called efficiency depends on the difference in intensity between the object and its image. It represents the efficiency of the lens in reproducing an image for the object being imaged. The two parameters which are studied are the diameter of the

virtual lens and the minimum required resolution for the calculated image. As the diameter of the virtual lens is varied the efficiency alternates between a maximum and a minimum values. Also, the amplitude of oscillation saturates as the diameter increase. The rate of saturation is proved to obey an exponential function. The increase in the diameter of the lens increases the amount of scattered waves which are collected by the lens from the object and so the lens is more capable to focus an accurate image for the object being imaged [5]. The frequency by which the efficiency oscillates is further studied by finding an equation for the frequency at which the oscillation happens. Studying the characteristics of varying the diameter of the virtual lens enables us to make best use of it in producing images with better quality and efficiency.

REFERENCES

[1] Hassanein, A M D E. "A Virtual Confocal Microscope with Variable Diameter to Improve Resolution." Journal of Multidisciplinary Engineering Science and Technology (JMEST) 2.3 (2015). ACCEPTED.

[2] KUBÍNOVÁ, L., J. JANÁCEK, P. KAREN, B. RADOCHOVÁ, F. DIFATO, and I. KREKULE. "Confocal Stereology and Image Analysis: Methods for Estimating Geometrical Characteristics of Cells and Tissues from Three-Dimensional Confocal Images." Physiol. Res. (Suppl. 1) 53 (2004): S47-55.

[3] Rector, David M., Douglas M. Ranken, and John S. George. "High-performance Confocal System for Microscopic or Endoscopic Applications." Methods 30.1 (2003): 16-27.

[4] Claxton, Nathan S., Thomas J. Fellers, and Michael W. Davidson. "Laser Scanning Confocal Microscope." CONFOCAL MICROSCOPY, 04 Mar. 2015. http://www.olympusconfocal.com/theory/LSCMIntro.pdf

[5] Hassanein, A M D E, Imaging Techniques Using Ultra Wide Band, PhD Thesis, University of Oxford, 2009.

[6] Keller, H. E. "Objective Lenses for Confocal Microscopy." Handbook of Biological Confocal Microscopy. Ed. James B. Pawley. Third ed. New York, NY: Springer, 2005.

[7] Tsuchida, Hirofumi, Shuichiro Ogasawara, and Kimiaki Yamamoto. "Characteristics of a Lens System Using Low-Dispersive Radial Gradient-Index Material." Optical Review 7.4 (2000): 337-40.

[8] Takeda, Minoru, Shinpei Okuda, Tsutomu Inoue, and Kento Aizawa. "Focusing Characteristics of a Spiral Plasmonic Lens." Japanese Journal of Applied Physics 52.9S2 (2013): 09LG03.

[9] Kim, Won-Gyum, Nam-Won Moon, Manoj Kumar Singh, Hwang-Kyeom Kim, and Yong-Hoon Kim. "Characteristic Analysis of Aspheric Quasi-optical Lens Antenna in Millimeter-wave Radiometer Imaging System." Applied Optics 52.6 (2013): 1122.

[10] Goodman, J W, Introduction to Fourier Optics, NewYork, McGraw-Hill, 1996.